αvβ6 Integrin Promotes the Invasion of Morphoeic Basal Cell Carcinoma through Stromal Modulation

Daniel Marsh,[1] Sarah Dickinson,[1] Graham W. Neill,[2] John F. Marshall,[1] Ian R. Hart,[1] and Gareth J. Thomas[1,3]

[1]Centre for Tumour Biology, Institute of Cancer, [2]Cutaneous Research, Institute of Cell and Molecular Sciences, [3]Clinical and Diagnostic Oral Sciences, Institute of Dentistry, Bart's and The London School of Medicine and Dentistry, London, United Kingdom

Abstract

Basal cell carcinoma (BCC) is the most prevalent cancer in the Western world and its incidence is increasing. The pathogenesis of BCC involves deregulated Sonic hedgehog signaling, leading to activation of the Gli transcription factors. Most BCCs have a nodular growth pattern, and are indolent, slow-growing, and considered "low-risk" lesions. In contrast, the "high-risk" morphoeic variant, which causes significant morbidity, has an infiltrative growth pattern, and is so-called because of its densely fibrous stroma. As αvβ6 is capable of promoting both carcinoma invasion and fibrosis, we examined the expression of this integrin in BCCs and found that the morphoeic type showed significantly higher αvβ6 expression than the nodular type (P = 0.0009). In order to examine the function of αvβ6, we transfected the transcription factors Gli1 or Gli2 into NTERT, human keratinocytes to generate a BCC model. These cells expressed αvβ6 and were invasive, although inhibition of αvβ6 had no direct effect on cell invasion. However, the cells showed αvβ6-dependent activation of transforming growth factor-β1, which induced transdifferentiation of human fibroblasts into myofibroblasts. Paracrine secretion of hepatocyte growth factor/scatter factor by these myofibroblasts promoted c-Met–dependent tumor invasion in both Transwell and three-dimensional organotypic assays. These experimental *in vitro* findings were confirmed using human clinical samples in which we showed that the stroma of morphoeic BCC is myofibroblast-rich compared with nodular BCC (P = 0.0036), that myofibroblasts express hepatocyte growth factor/scatter factor, and that morphoeic BCCs are strongly c-Met–positive. These data suggest that αvβ6-dependent transforming growth factor-β1 activation induces both the infiltrative growth pattern and fibrotic stroma so characteristic of morphoeic BCC. [Cancer Res 2008;68(9):3295–303]

Introduction

Basal cell carcinoma (BCC) is the most common cancer in the Western world, and its incidence is increasing worldwide by up to 10% a year (1, 2). In the United States, the incidence of BCCs has doubled approximately every 14 years, with an estimated one million new cases annually (3). BCCs rarely metastasize however, and although patient mortality is low, these tumors are locally invasive, and may cause significant tissue destruction and morbidity, particularly because ~80% of tumors occur on the head and neck (4). The pathogenesis of BCC involves deregulated Sonic hedgehog signaling (Shh), leading to the activation of the glioma-associated (Gli) family of zinc finger transcription factors (5). In human disease, this is often due to inactivation mutations in the hedgehog receptor and antagonist, PTCH1 (6). Transgenic mouse models have confirmed the importance of Shh signaling in BCC development; loss of Ptch1 function from the basal keratinocytes of mouse skin is sufficient to induce BCC-like tumor formation (7). Conversely, mice overexpressing mediators of Shh signaling (including Shh, Gli1, and Gli2) also develop tumors resembling BCC (8–10).

BCCs are morphologically diverse and a number of different histologic subtypes have been described. The most common BCC variant is the nodular subtype, which accounts for ~80% of tumors (4); these are composed of well-defined cellular islands and are regarded as "low-risk" being, typically, indolent and slow-growing. In contrast, ~6% of BCCs comprise the "high-risk" morphoeic (sclerosing, fibrosing, scirrhous) variant, which occurs mostly on the face/head and neck. This type has a more aggressive natural history and is prone to recurrence (4, 11). In contrast with nodular BCC, such tumors have an infiltrative growth pattern composed of small islands and strands of neoplastic cells embedded in a densely fibrous stroma.

The epithelial-specific integrin αvβ6 is usually not detectable on normal adult epithelia but is up-regulated during tissue remodeling, including wound healing and carcinogenesis (12, 13). αvβ6 has several ligands, which include the matrix proteins fibronectin and tenascin (13), and binds to the latency-associated peptide of transforming growth factor-β1 (TGF-β1) and TGF-β3 resulting in activation of the cytokines; a process implicated in pathogenic organ fibrosis (14, 15).

Increasingly, αvβ6 overexpression has been reported in numerous types of carcinoma in which it seems to have a tumor-promoting effect (16–21). High expression in colon, lung, and cervical carcinomas correlates with poor patient survival (18, 20, 21), and studies have shown that αvβ6 may modulate several cell functions associated with tumor progression (16–19, 22, 23). We have previously shown that αvβ6 promotes invasion in head and neck squamous cell carcinoma (SCC) *in vitro* and *in vivo*, and recently described a novel link between the integrin and the cyclooxygenase-2 metabolite prostaglandin E_2 in modulating proinvasive Rac1 activation (16, 17, 19). Bates et al. (18) reported increased αvβ6 expression in colon carcinoma cells that had undergone epithelial-mesenchymal transition (EMT) and suggested that activation of TGF-β1 by αvβ6 provided a mechanism to sustain EMT. Therefore, it seems that αvβ6 may promote tumor invasion directly through several different mechanisms.

Note: Supplementary data for this article are available at Cancer Research Online (http://cancerres.aacrjournals.org/).

D. Marsh and S. Dickinson contributed equally to this work.

Requests for reprints: Gareth J. Thomas, Centre for Tumour Biology, Institute of Cancer, Bart's and The London School of Medicine and Dentistry, London EC1M 6BQ, United Kingdom. Phone: 44-20-7014-0409; Fax: 44-20-7014-0401; E-mail: gareth.thomas@cancer.org.uk.

doi:10.1158/0008-5472.CAN-08-0174

Here, we show that αvβ6 is expressed at low levels in low-risk nodular BCC but is markedly up-regulated in the more infiltrative morphoeic variant. We transfected the transcription factors Gli1 or Gli2 into NTERT, human keratinocytes (24) to generate a BCC model. Surprisingly, and in contrast to our work with SCC, we found that αvβ6 did not directly promote Transwell cell invasion. However, αvβ6-dependent activation of TGF-β1 did modulate stromal fibroblast-to-myofibroblastic transdifferentiation. Myofibroblasts in turn promoted BCC invasion through up-regulated paracrine secretion of hepatocyte growth factor/scatter factor (HGF/SF). Using human clinical samples, we confirmed these *in vitro* findings and showed that the stroma of morphoeic BCC is myofibroblast-rich compared with nodular BCC, that myofibroblasts express HGF/SF, and that morphoeic BCCs are strongly c-Met–positive. These data suggest that αvβ6 may promote invasion through indirect stromal mechanisms, and that αvβ6-dependent TGF-β1 activation might explain both the infiltrative growth pattern and fibrotic stroma of morphoeic BCC.

Materials and Methods

Antibodies and reagents. The monoclonal antibodies (mAb) used in this study were as follows: 10D5, anti-αvβ6 integrin was from Chemicon International; 6.2G2, and 6.3G9, anti-human αvβ6 integrin were generously provided by Dr. S. Violette (BiogenIdec, Cambridge, MA). 53a2 rat mAb against human αvβ6 was produced in-house. mAbs to c-Met (Invitrogen), E-cadherin (Santa Cruz Biotechnology), HGF/SF (R&D Systems), smooth muscle actin (SMA; IA4, Dako), and cytokeratin (AE1/AE3; Dako) were purchased commercially. Polyclonal antibody C-19 antihuman integrin β6 was from Santa Cruz Biotechnology. Human type 1 collagen was obtained from Sigma, Matrigel was from BD Biosciences, and MET kinase inhibitor SU11274 was from Calbiochem.

Immunohistochemistry. Antibodies used were anti-αvβ6 (6.2G2, 0.5 μg/mL; Biogen Idec), anti-SMA (IA4, 1;100; Sigma), anti–c-Met (1:50; Zymed) anti-HGF/SF (1:10; R&D Systems), anticytokeratin (AE1/AE3, 1:50; Dako), or anti–E-cadherin (1:50; Santa Cruz Biotechnology). Antigen retrieval varied according to primary antibody: 0.1% α-chymotrypsin and 0.1% calcium chloride (pH 7.8) for 20 min at 37°C (AE1/AE3), Digest-All 3 Pepsin Solution (Zymed Laboratories) for 5 min at 37°C (6.2G2), and microwaving for 30 min in 0.1 mol/L citrate buffer (pH 6; c-Met, SF/HGF, E-cadherin). Endogenous peroxidase was neutralized with 0.45% hydrogen peroxidase in methanol for 15 min and primary antibodies were applied in TBS (pH 7.6) for 1 h. Antimouse IgG biotinylated secondary antibody (Vectastain Elite ABC Reagent, Vector Laboratories) was applied for 30 min followed by peroxidase-labeled streptavidin (Vectastain Elite ABC Reagent, Vector Laboratories) for 30 min. Peroxidase was visualized using DAB+ (Dako) for 7 min and counterstained in Mayer's hematoxylin (Sigma).

Fifteen nodular BCC and 13 morphoeic BCC were selected from archival material and stained for αvβ6, SMA, c-Met, HGF/SF, E-cadherin, and cytokeratin, then scored according to the Quickscore method as previously described (25). Appropriate ethical approval was obtained. The staining intensity of αvβ6 and SMA was scored on a scale of 1 to 3 (1, weak; 2, moderate; and 3, strong), and the proportion of cells staining positively was scored on a scale of 1 to 4 (1, <25%; 2, 25–50%; 3, 51–75%; and 4, 76–100%). The score for intensity was added to the score for proportion to give a score in the range of 0 to 7 and grouped as score = 0 (−), score = 1–3 (+), score = 4–5 (++), or score = 6–7 (+++).

Cell culture. To generate a BCC model, the coding sequences of GLI1 and an active mutant of GLI2 (ΔN-GLI2b) were cloned into pBabePuro and retroviral particles were made using the Phoenix (amphotropic) packaging cell line as described previously (26). NTert-1 keratinocytes (NTGli1 and NTGli2) were selected with puromycin (1 μg/mL) 48 h after retroviral transduction (for 72 h) and Gli expression was confirmed by Western blot analysis (GLI1 C18 and GLI2 H-300 abs; Santa Cruz Biotechnology). Cells were grown in keratinocyte growth medium (16). Human fetal foreskin fibroblasts (HFFF2, American Type Culture Collection) were maintained in fibroblast growth medium (DMEM supplemented with 10% FCS) at 37°C in a humidified atmosphere.

RNAi. RNAi SMART pool reagents targeting β6 and control (random) sequences were obtained from Dharmacon and used as described previously (19). Cells were seeded into six-well plates and left for 24 h until ~40% confluent, then transfected with 100 nmol/well of the relevant duplex pool using Oligofectamine transfection reagent (Invitrogen). Cells were used in assays after 24 to 48 h. Cells also were lysed and used to verify protein knockdown by Western blotting analysis.

Flow cytometry. Flow cytometry was performed (16) using anti-αvβ6 antibody (10D5; Chemicon), anti–c-Met antibody (Invitrogen), and Alexafluor 488–conjugated secondary antibody (Molecular Probes). Negative controls used secondary antibody only. Labeled cells were scanned on a FACSCalibur cytometer (BD Biosciences) and analyzed using CellQuest software, acquiring 1×10^4 events. Results show mean fluorescence (arbitrary units, log scale).

TGF-β bioassay. Mink lung epithelial reporter cells stably expressing a TGF-β–responsive luciferase reporter construct (27) were plated overnight in 96-well plates in DMEM, 10% FCS (5×10^4 cells/well). The medium was changed to serum-free α-MEM, and NTGli1 or NTGli2 cells (2.5×10^4 cells/well) were added to each well in serum-free α-MEM containing anti-αvβ6 antibody (10 μg/mL, 10D5; Chemicon) or control antibody (10 μg/mL, mouse monoclonal anti-α4 integrin, mAb7.2; produced in-house). The cells were cocultured overnight, washed once in PBS, and lysed in reporter lysis buffer (Promega). Luciferase assay buffer (Promega) was added to the supernatant and the luminescence measured using a Wallac plate reader.

Coculture experiments. HFFF2 cells and NTGli1 or NTGli2 cells were plated in six-well dishes (2.5×10^5 cells of each cell type) or onto 13-mm glass coverslips in 24-well plates (2.5×10^4 cells of each cell type). Cells were seeded in DMEM, 10% FCS ±antibodies (as above), or TGF-β1 (1 ng/mL; R&D Systems) and left to attach. The medium was then changed to serum-free DMEM containing antibodies or TGF-β and cultured for an additional 48 h. The cells were either lysed for analysis by Western blotting or fixed and processed for immunofluorescence. The supernatant was analyzed by ELISA for HGF/SF.

Western blot analysis. Cells were lysed in NP40 buffer (Biosource). Samples containing equal amounts of protein were electrophoresed under reducing conditions in 12% SDS-PAGE gels. Protein was electroblotted to nitrocellulose membranes (Amersham Biosciences). Blots were probed with antibodies against αvβ6 (Santa Cruz Biotechnology) or SMA (Dako). Horseradish peroxidase–conjugated anti-goat or anti-mouse (Dako) were used as secondary antibodies. Bound antibodies were detected with the enhanced chemiluminescence Western blotting detection kit system (Amersham). Blots were probed for HSC70 (Santa Cruz Biotechnology) as a loading control. Exposures of blots in the linear range were quantified by densitometry software (Scion Corp.).

Confocal microscopy. Cells were fixed for 10 min in 4% formaldehyde in cytoskeletal buffer (10 mmol/L MES, 3 mmol/L $MgCl_2$, 138 mmol/L KCl, 2 mmol/L EGTA; pH 6.1) with 0.32 mol/L of sucrose. Cells were permeabilized for 5 min with 0.2% Triton X-100 and incubated for 30 min in DMEM, 0.1% bovine serum albumin, and 0.1% sodium azide. Nonspecific staining was blocked by incubation in 5% normal goat serum. Cells were then incubated with anti-SMA (IA4; Dako) and anti-αvβ6 antibodies (53a.2; in-house) for 1 h, and binding detected by incubation with secondary antibodies conjugated with Alexafluor 488 (Molecular Probes) or Cy3 (Jackson ImmunoResearch) for 45 min. Nuclei were visualized using 4′,6-diamidino-2-phenylindole (Invitrogen). Coverslips were mounted onto glass slides using Mowiol. All dilutions were in DMEM, 0.1% bovine serum albumin, and 0.1% sodium azide and incubations were at room temperature. Images were recorded and processed with a confocal laser scanning microscope (Zeiss LSM510).

Preparation and use of medium conditioned by fibroblasts and myofibroblasts. Fibroblasts (5×10^5) were plated in fibroblast growth medium in 75 cm^2 culture flasks for 24 h, then washed twice with PBS. To induce a myofibroblastic phenotype, cells were incubated for 48 h in

medium containing recombinant TGF-β1 (1 ng/mL; R&D Systems), which was acid-activated prior to use (4 mmol/L HCl/0.1% bovine serum albumin). Control cells were cultured in medium alone. After 48 h, the cells were washed twice with PBS, and cultured for a further 72 h in α-MEM. The control fibroblast-conditioned medium (FCM) or myofibroblast-conditioned medium (MCM) was collected, clarified by centrifugation, and the cells detached and counted. The volumes of FCM and MCM were corrected for equivalent number of cells per milliliter of medium, and 500 μL was placed in the lower chamber of a Transwell invasion assay as a chemoattractant.

Transwell invasion assays. Cell invasion assays were performed over 72 h using Matrigel-coated (diluted 1:2 in α-MEM) polycarbonate filters (Transwell, BD Biosciences; ref. 17). Cells invading the lower chamber were trypsinized and counted on a Casy 1 counter (Sharfe System GmbH). Results were expressed relative to invasion of control treatment (100). For blocking experiments, anti-αvβ6 antibody (6.3G9; 10 μg/mL) or control antibody (mAb7.2; 10 μg/mL) was added to the cells for 30 min prior to plating. For c-Met inhibition, cells were treated with c-Met kinase inhibitor, SU11274 (5 μmol/L; Calbiochem), for 24 h prior to use and the inhibitor was present throughout the experiment.

Organotypic culture. Organotypic cultures with an air-tissue interface were prepared as described (28). Gels comprised a 50:50 mixture of Matrigel (Becton Dickinson) and type I collagen (Upstate) containing 5×10^5/mL of HFFF2 cells, to which 5×10^5 NTGli1 cells were added. Experiments were also carried out by adding a mixture of NTGli1 cells and HFFF cells to a cell-free gel. Each method gave similar results. For inhibition studies, SU11274 (5 μmol/L) was added to the keratinocyte growth medium. The medium was changed every 2 days. After 6 days, the gels were bisected, fixed in formal saline, and processed to paraffin. Sections (4 μm) were immunostained with the pan-cytokeratin antibody AE1/AE3 (Dako).

Statistical analysis. Data are expressed as the mean ± SD of a given number of observations. Where appropriate, one-way ANOVA was used to compare multiple groups. Comparisons between groups were made with Fisher's PLSD. $P < 0.05$ was considered to be significant. Figures show representative examples of independent repeats with error bars representing SD.

Results

αvβ6 expression is significantly higher in the morphoeic variant BCC. Morphoeic BCCs have an infiltrative growth pattern and a densely fibrous stroma compared with nodular BCCs. Because αvβ6 is capable of promoting both invasion and fibrosis, we examined the expression and distribution of integrin in these BCC subtypes using immunochemistry (results are summarized in Table 1). Of 15 nodular BCC examined, strong expression (+++) of αvβ6 was present in 7% of tumors. In contrast, expression of αvβ6 in morphoeic BCC was significantly higher ($P = 0.0009$) with 10 of 13 tumors (77%) expressing the integrin strongly (Table 1; Fig. 1*A*). No strong αvβ6 staining was observed in the epidermis of normal skin (data not shown).

Generation of NTGli1 and NTGli2 keratinocytes. Because αvβ6 is a proinvasive integrin (16–18), the marked differences in αvβ6 expression between BCC variants suggested that the integrin may play a role in generating a more aggressive tumor phenotype. To study the role of αvβ6 in BCC, we first had to generate an *in vitro* model of the disease. Abnormal activation of the Shh signaling pathway is a major contributing factor in the development of BCCs (5). cDNAs encoding the Shh transcription factors Gli1 and Gli2 (DN-GLI2b) were retrovirally transduced into NTert-1 skin keratinocytes (24) and expression of the proteins was confirmed using Western blotting (Fig. 1*B*).

αvβ6 does not promote NTGli1 Transwell invasion. Keratinocyte-derived cell lines (and primary keratinocyes) usually express αvβ6 in culture (13). Flow cytometry and confocal microscopy confirmed that NTGli1 and NTGli2 cells expressed αvβ6 (Fig. 1*C*; data not shown); however, transduction of Gli1 or Gli2 did not upregulate the expression of αvβ6 or significantly alter the expression of other integrins (Supplementary Fig. S1*A*). We then assessed the effect of inhibiting αvβ6 on the ability of NTGli1 and NTGli2 cells to invade Matrigel. Inhibition of αvβ6 using antibodies (6.3G9) or β6 RNAi did not suppress the invasion of NTGli1 ($P = 0.834$ and $P = 0.718$, respectively; Fig. 1*D*). NTGli2 cells invaded similarly (Supplementary Fig. S1*B*). In contrast, and as we have shown previously, antibody inhibition of αvβ6 expressed by carcinoma cells derived from the head and neck (VB6), breast (BT20), and lung (H441) reduced invasion significantly ($P = 0.0035$, $P = 0.005$, and $P = 0.002$, respectively). Because it also has been suggested that αvβ6 may promote invasion directly through modulating TGF-β1–dependent EMT, we repeated the invasion assays adding TGF-β1 into the assay or inhibiting TGF-β1 signaling using recombinant soluble TGF-β receptor II (rsTGF-βRII). Neither treatment had an effect on NTGli1 invasion ($P = 0.52$ and $P = 0.47$, respectively; Fig. 1*D*).

αvβ6 modulates TGF-β1 activation in NTGli1 cells. αvβ6 modulates several cell functions, including activation of TGF-β1 (14). To investigate whether αvβ6 activated TGF-β1 in NTGli1 cells, we carried out a TGF-β bioassay as described previously (27).

Table 1. αvβ6 and SMA expression in nodular and morphoeic BCCs

	Cases	αvβ6 and SMA expression									
		−		+		++		+++		+++ (%)	
		αvβ6	SMA	αvβ6	SMA	αvβ6	SMA	αvβ6	SMA	αvβ6	SMA
Nodular BCC	15	3	2	2	1	9	6	1	6	7	40
Morphoeic BCC	13	0	0	1	0	2	2	10	11	77	85

NOTE: Fifteen nodular BCCs and 13 morphoeic BCCs were selected stochastically and stained for αvβ6 and SMA before being scored according to the Quickscore method (24). Briefly, the staining intensity was scored on a scale of 1 to 3 (1, weak; 2, moderate; 3, strong), and the proportion of the tumor or stromal cells staining positively was scored on a scale of 1 to 4 (1, <25%; 2, 25–50%; 3, 51–75%; and 4, 76–100%). The score for intensity was added to the score for proportion to give a score in the range of 0 to 7 and grouped as score = 0 (−), score = 1–3 (+), score = 4–5 (++), or score = 6–7 (+++). There was a significantly higher expression of αvβ6 and SMA in morphoeic BCCs compared with nodular BCCs ($P = 0.0009$ and $P = 0.0036$, respectively).

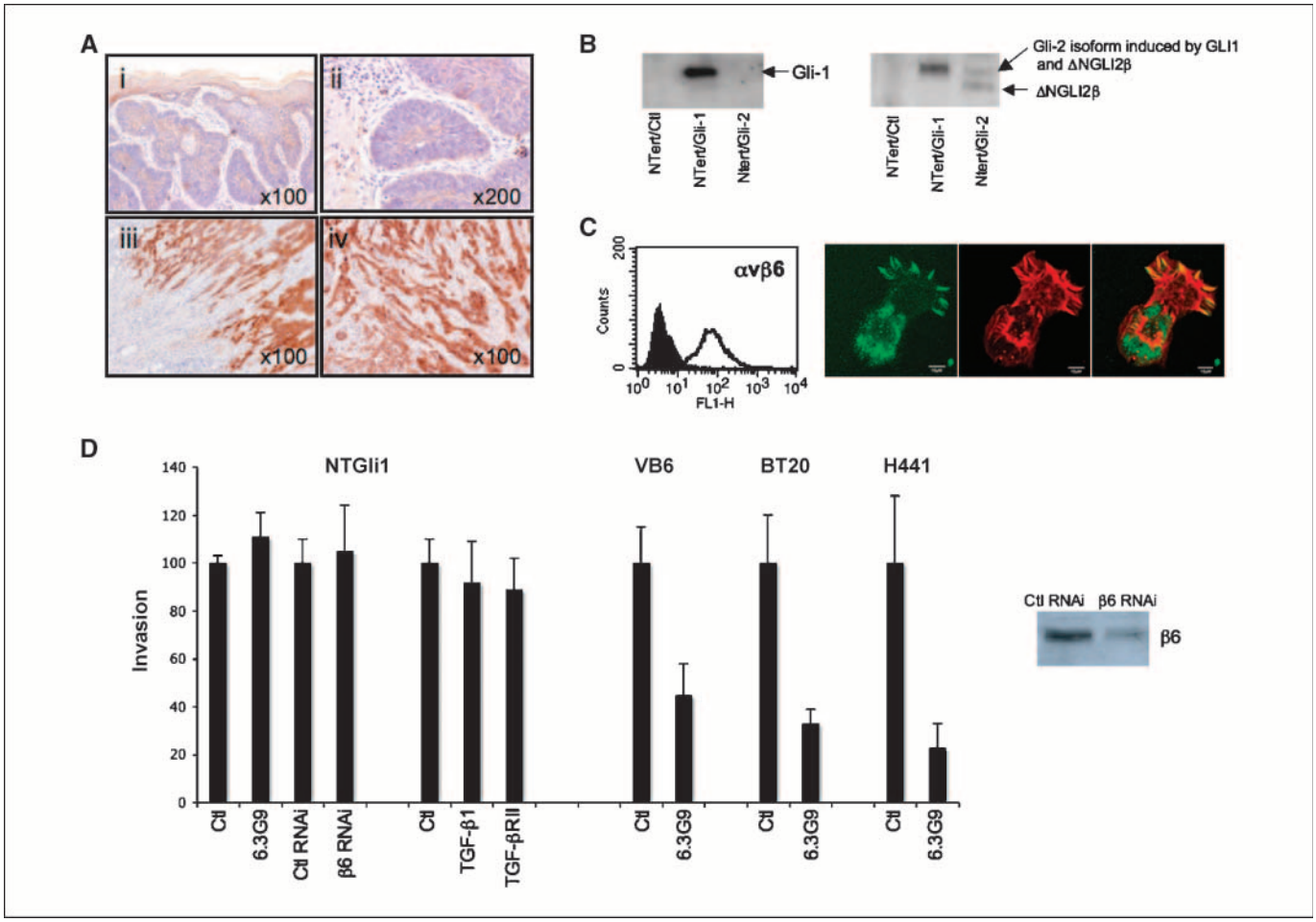

Figure 1. *A,* immunohistochemistry showing representative αvβ6 expression in nodular BCC (*i* and *ii*) and morphoeic BCC (*iii* and *iv*). αvβ6 expression was significantly higher in morphoeic BCC ($P = 0.0009$). *B,* NTert keratinocytes were transfected with GLI1 and GLI2 cDNA and protein expression confirmed by Western blotting. *C,* flow cytometry analysis showed αvβ6 expression by NTGli1 cells. This was confirmed by confocal microscopy. Confocal micrograph shows αvβ6 staining (*green*), actin (*red*), and merged images. *D,* Transwell invasion of NTGli1 cells was not inhibited by blockade of αvβ6 integrin (*6.3G9*) or by transient transfection of cells with β6 RNAi. Treatment of NTGli1 cells with TGF-β1 or inhibition of TGF-β1 using recombinant soluble TGF-β receptor type II (*TGF-βRII*) did not affect invasion. In contrast, inhibition of αvβ6 in head and neck (*VB6*), breast (*BT20*), and lung (*H441*) carcinoma cells inhibited invasion significantly ($P = 0.0035$, $P = 0.005$, and $P = 0.002$, respectively). Results are expressed relative to control invasion (= 100). Western blotting confirmed RNAi-knockdown of β6 protein at 72 h (~95%).

Inhibition of αvβ6 using antibodies (10D5) or β6 RNAi significantly reduced TGF-β1 activation (by 59% and 37%, respectively; $P \leq 0.0001$ and $P = 0.0006$; Fig. 2*A*). NTGli2 cells activated TGF-β1 similarly (Supplementary Fig. S1*C*).

A common finding in many types of carcinoma is that stromal fibroblasts become "activated" myofibroblasts and express a number of contractile proteins, particularly α-SMA (29), and TGF-β1 is considered to have a central role in inducing this myofibroblastic phenotype (30). To determine whether NTGli1 cells could induce myofibroblast differentiation, we carried out coculture experiments with HFFF2 cells. HFFF2 cells express low levels of SMA in culture (Fig. 2*C*). Coculture of HFFF2 with NTGli1 cells induced myofibroblast transdifferentiation, producing a significant increase in SMA expression (Fig. 2*B* and *C*), which was associated with cytoplasmic stress fibers (Fig. 2*B*). To show that myofibroblast generation was αvβ6-dependent, we repeated coculture assays in the presence of an αvβ6-inhibitory antibody. When the αvβ6 antibody was included, SMA expression was inhibited significantly (Fig. 2*B*). This was confirmed by Western blotting ($P = 0.006$; Fig. 2*C*).

Myofibroblasts promote NTGli1 invasion. We have shown previously that myofibroblasts promote the invasion of SCC cells through paracrine secretion of growth factors (25). Although expression of αvβ6 did not modulate the invasion of NTGli1 cells directly, we postulated that the generation of a stromal myofibroblastic phenotype could have an invasion-promoting effect. To determine the effect of myofibroblasts on NTGli1 cell invasion, we performed Transwell invasion assays through Matrigel. Myofibroblasts were generated by treating HFFF2 cells with TGF-β1 and then cultured for 72 hours in α-MEM. The MCM was used as a chemoattractant in the lower chamber of the Transwell, and NTGli1 cells were allowed to invade towards this stimulus for 72 hours before being counted. Untreated FCM was used for comparison. We show that MCM significantly promoted the invasion of NTGli1 cells compared with FCM ($P \leq 00001$; Fig. 3*A*). The addition of αvβ6-inhibitory antibody (6.3G9) into the Transwell assay did not inhibit invasion (Fig. 3*A*).

To further investigate the interaction between NTGli1 and HFFF2 cells in the invasive process, we used an organotypic invasion model (15). In contrast with Transwell invasion, transient

transfection of NTGli1 cells with β6 RNAi markedly suppressed invasion (Fig. 3*B*). This suggested that the invasion-promoting effect of αvβ6 was modulated indirectly through HFFF2 cells.

Myofibroblasts up-regulate HGF/SF which promotes NTGli1 invasion. Previously, studies have shown that myofibroblasts secrete HGF/SF (31). This cytokine promotes epithelial cell growth and migration and has been shown to stimulate invasion in squamous carcinoma cells (25). To determine whether induction of a myofibroblastic phenotype was associated with increased production of HGF/SF, we examined conditioned medium from cocultures of NTGli1 and HFFF2 cells treated with control or anti-αvβ6 inhibitory antibodies. Figure 4*A* shows that coculture of NTGli1 and HFFF2 induced HGF/SF production, which was suppressed when αvβ6 was inhibited.

To determine whether the invasion-promoting effect of MCM was modulated through HGF/SF, we inhibited the HGF/SF signaling pathway in NTGli1 cells using the Met kinase inhibitor, SU1224 (5 μmol/L; Calbiochem). Flow cytometry confirmed that NTGli1 cells expressed the HGF/SF receptor, c-Met (Fig. 4*B*). Inactivation of c-Met significantly reduced the invasion of NTGli1

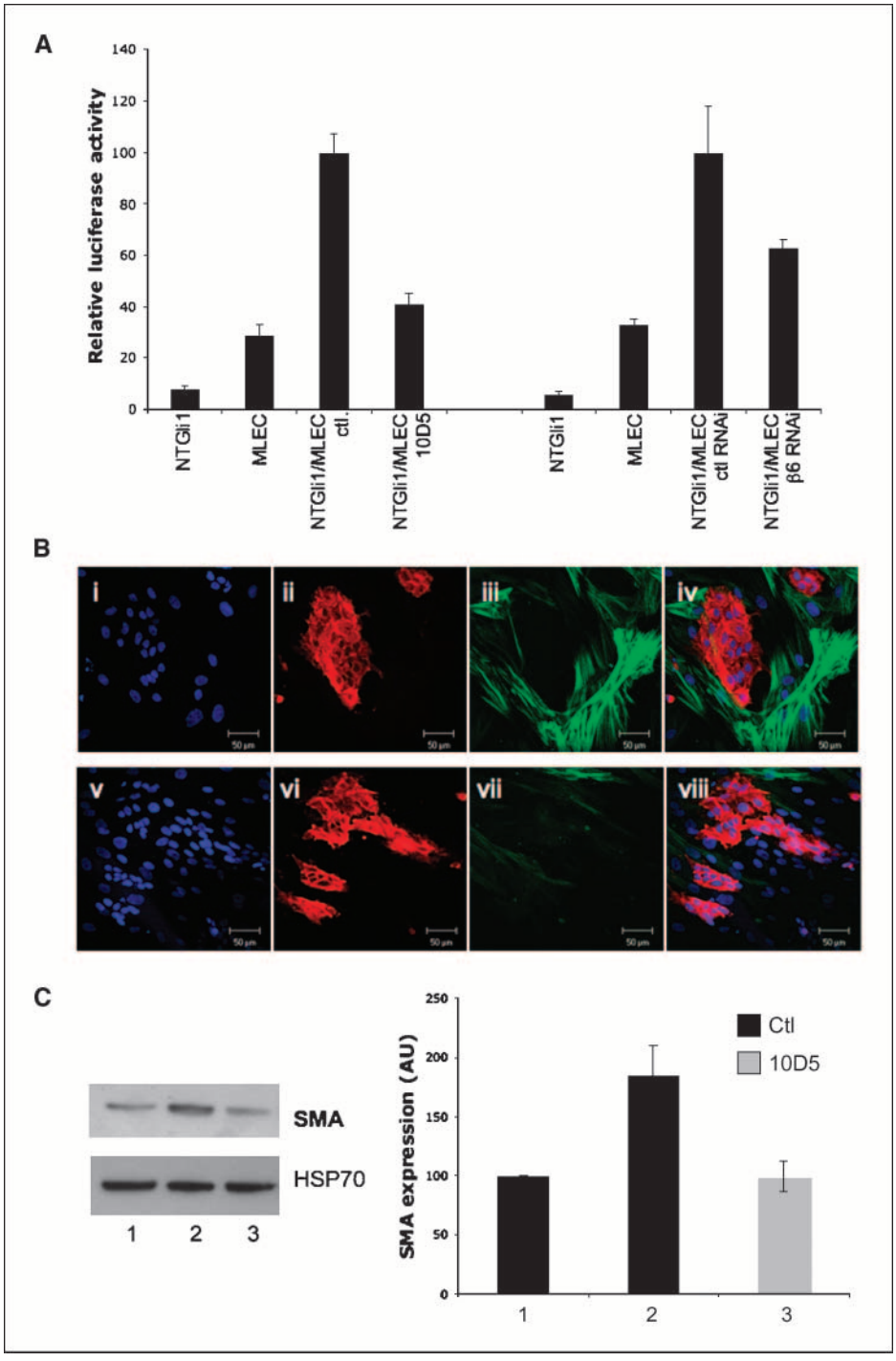

Figure 2. *A,* TGF-β activation coculture assay. Coculture of NTGli1 with mink lung epithelial reporter cells (*MLEC*) promoted TGF-β activation, which was suppressed by antibody blockade of αvβ6 integrin (*10D5*) or by transient transfection of cells with β6 RNAi. Control antibody was anti-α4 integrin, 7.2. *B,* HFFF2 cells and NTGli1 cells were cocultured on glass coverslips and treated with control (7.2; *i–iv*) or anti-αvβ6 (10D5; *v–viii*) antibodies. Confocal micrograph shows cell nuclei (*blue; i* and *v*), αvβ6-positive NTGli1 cells (*red; ii* and *vi*), SMA-positive myofibroblasts (*green; iii* and *vii*), or the combined images (*right; iv* and *iii*). When cocultured with NTGli1, HFFF2 cells up-regulated SMA indicating myofibroblastic transdifferentiation (*i–iv*). When αvβ6 was inhibited, no myofibroblastic phenotype was produced (*v–viii*). *C,* Western blotting showing low level of basal SMA expression in HFFF2 cells (*lane 1*), SMA induction on coculture with NTGli1 cells (*lane 2*), and suppression of SMA induction when cocultured with NTGli1 cells in the presence of an αvβ6-inhibitory antibody (*10D5; lane 3*). Histogram represents the combined results of Western blot densitometric analysis from three individual experiments.

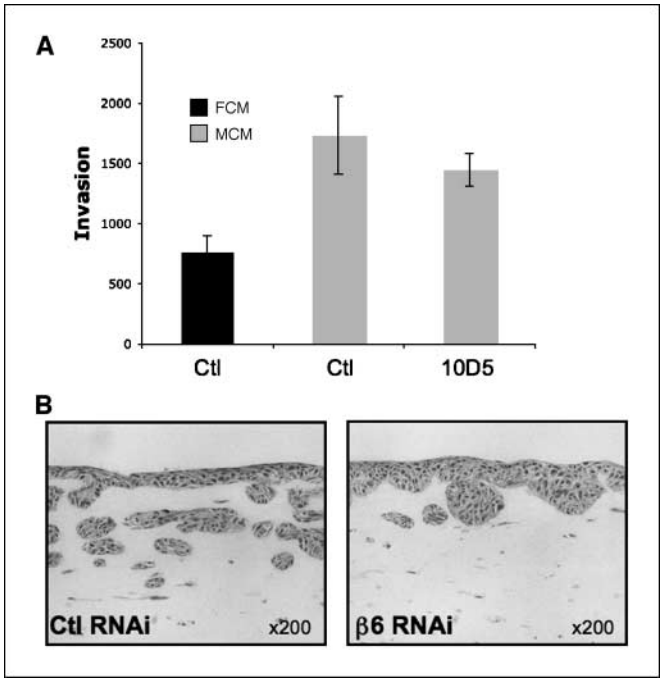

Figure 3. *A,* Transwell invasion assay using conditioned medium from fibroblasts (*FCM*) or myofibroblasts (*MCM*) as a chemoattractant in the lower chamber of the Transwell. MCM significantly promoted the invasion of NTGli1 cells. Blockade of αvβ6 (10D5) did not inhibit MCM-induced invasion. *B,* NTGli1 cells were transiently transfected with random or β6 RNAi and then grown in organotypic culture with HFFF2 cells for 6 days. In contrast with Transwell invasion, inhibition of αvβ6 suppressed the invasion of NTGli1 cells.

cells towards MCM (P = 0.00002; Fig. 4*B*). Following c-Met inhibition, the level of invasion was similar to that produced by FCM, suggesting that the invasion-promoting effect of MCM was mediated by HGF/SF (Fig. 4*B*). SU1124 also inhibited NTGli1 invasion in organotypic cultures, although the inhibitory effect was not as marked as that produced using β6 RNAi (Fig. 4*C*).

The stroma of morphoeic BCC is myofibroblast-rich. Our *in vitro* data predicted that the stroma of morphoeic BCC would be rich in myofibroblasts producing HGF/SF. To determine whether this stroma contained myofibroblasts, we immunostained nodular and morphoeic BCC for SMA expression (results are summarized in Table 1). Similar to αvβ6, expression of SMA was significantly higher in morphoeic BCCs (P = 0.0036) with 11 of 13 tumors (85%) having stroma with strong SMA expression, indicating myofibroblastic differentiation (Fig. 5*A, i* and *ii*). In contrast, only 6 of 15 nodular BCCs (40%) showed strong SMA expression (Fig. 5*A, iii* and *iv*). No SMA staining was observed in the dermis of normal skin (data not shown).

Morphoeic BCC express c-Met and HGF/SF. Immunochemistry confirmed that c-Met was strongly (+++) or moderately (++) expressed by all morphoeic BCCs (Fig. 5*B, i* and *ii*) and that HGF/SF was commonly detected in myofibroblasts in the desmoplastic stroma (Fig. 5*B, iii* and *iv*). Interestingly, nodular BCC also expressed c-Met strongly and expression did not differ significantly from the morphoeic variants (P = 0.69; Supplementary Fig. S2*A*). Normal epidermis was c-Met–negative or showed weak expression in basal keratinocyes only (Supplementary Fig. S2*A*).

Discussion

BCC is the most common human cancer and its incidence is increasing worldwide. Although most BCC are indolent and slow-growing, several aggressive histologic variants exist which cause significant morbidity. Expression of αvβ6 occurs in many carcinoma types in which experimental studies indicate that it promotes an invasive phenotype (16, 17, 19). Here, we show that the integrin αvβ6 is expressed at significantly higher levels in aggressive, infiltrative morphoeic BCC compared with more common nodular BCC. Using Gli-transfected NTert human skin keratinocytes as a BCC model, we examined the effects of αvβ6 expression in these cells. Inhibition of αvβ6 had no direct effect on cell invasion of Matrigel. However, in coculture assays, NTGli1 cells induced human fibroblast-to-myofibroblast transdifferentiation through αvβ6-dependent activation of TGF-β1. We show that the fibrotic stroma of morphoeic BCC is myofibroblast-rich compared with nodular BCC, and that myofibroblasts promote BCC invasion through up-regulated paracrine secretion of HGF/SF.

Morphoeic BCC account for ~6% of BCCs, and are so-called because of the their fibrotic (desmoplastic) stroma. Unlike the more common nodular BCC variant, morphoeic BCCs are aggressively infiltrative, resulting in greater depth of invasion, tissue destruction, and thus, greater frequency of recurrence (11). Because 95% of these tumors are located on the face or head, this causes significant morbidity (4). We found that 77% of morphoeic BCC expressed αvβ6 strongly. This was similar to expression levels in cutaneous SCC (66% high expression; 13 of 19 tumors),[4] but was significantly higher than nodular BCC (7%). Interestingly, the histologic growth pattern of morphoeic BCC more closely resembles SCC than nodular BCC.

Although the expression of αvβ6 has been increasingly described in numerous carcinoma types, and often correlates with poor prognosis (18, 20, 21), the mechanisms regulating expression remain to be fully described. The cytokines tumor necrosis factor-α and TGF-β1 (mediated by the transcription factor Ets-1) and high cell density have been previously reported to up-regulate this integrin (13, 18). Transfection of Gli1 and Gli2 into NTert-immortalized keratinocytes did not induce further up-regulation. Consistent with this finding, the β6 promoter does not contain the reported Gli-binding site (GACCACCCA; ref. 32).

We have previously shown that αvβ6 promotes the invasion of head and neck SCC *in vitro* and *in vivo* (16, 17, 19). These data suggest that αvβ6 is an attractive tumor target, and several studies have now inhibited tumor growth successfully *in vivo* using treatments directed against the integrin (33, 34). Surprisingly, inhibition of αvβ6 had no effect on NTGli1 cell Transwell invasion (Fig. 1*D*). However, αvβ6 modulates several cell functions including activation of TGF-β1 (14), and we found that activation of TGF-β1 in NTGli1 cells was αvβ6-dependent (Fig. 2*A*). The role of TGF-β1 in tumor biology is complex, having both suppressive and promoting effects (35). This is explained, in part, by observations that most carcinomas become refractory to the antiproliferative effect of TGF-β1 (35). TGF-β1 also has direct pro-oncogenic effects on tumor cells, including the promotion of motility through modulating EMT. However, treatment of NTGli1 cells with recombinant TGF-β1 or inhibition of TGF-β1 signaling using recombinant soluble TGF-βRII receptor had no effect on invasion.

[4] Unpublished data.

These data suggest that activation of TGF-β1 did not promote NTGli1 cell invasion directly.

Another mechanism by which αvβ6-dependent activation of TGF-β1 could promote tumor progression is by modulating the tumor stroma. TGF-β1 is considered to have a central role in inducing the myofibroblastic phenotype, and αvβ6-dependent activation of TGF-β1 results in the pathologic fibrosis of several epithelial organs (14, 15). There is now abundant evidence that the tumor stroma promotes tumor progression (36–38), and we have previously shown a proinvasive paracrine interaction between myofibroblasts and head and neck SCC cells (25). Transdifferentiation of myofibroblasts is frequently observed to be associated with the edge of an actively expanding tumor mass, and it is common to find αvβ6 expressed most strongly at this invasive margin (19, 25, 34). In coculture assays, we found that NTGli1 cells modulated myofibroblast transdifferentiation through αvβ6-dependent activation of TGF-β1, and that conditioned medium from myofibroblasts promoted NTGli1 Transwell invasion. Using immunochemistry, we confirmed that the stroma of morphoeic BCCs is myofibroblast-rich compared with nodular BCCs. Additionally, although inhibition of αvβ6 had no anti-invasive effect in Transwell assays, when NTGli1 cells were admixed with fibroblasts in organotypic culture, β6 RNAi knockdown markedly reduced invasion. We suggest that this effect was modulated through the suppression of myofibroblast transdifferentiation.

Myofibroblasts may promote tumor progression in a number of different ways including secretion of proteases, matrix proteins, and cytokines (38). Coculture of NTGli1 and HHF2 cells resulted in up-regulated secretion of HGF/SF, which was suppressed when αvβ6 was inhibited (Fig. 4*A*). HGF/SF acts through the c-Met tyrosine kinase receptor, and misregulated expression of both cytokine and receptor is a common finding in many tumor types (39), although expression has not been previously described in BCC. We found that inhibition of HGF/SF signaling suppressed the invasion-promoting effect of MCM in Transwell assays (Fig. 4*B*), and also inhibited invasion in organotypic culture (Fig. 4*C*). Inhibition of c-Met in organotypic cultures did not inhibit invasion as markedly as knockdown of β6 protein, suggesting that additional myofibroblastic products may be involved in the invasive process. De Wever and colleagues (40) found that myofibroblasts stimulated the invasion of colon carcinoma cells through secretion of a combination of HGF/SF and tenascin C, and it is possible that a similar mechanism promotes the invasion of NTGli1 cells. Immunochemistry showed that morphoeic BCC express both c-Met receptor and stromal HGF/SF (Fig. 5*B*). Interestingly, c-Met expression was also present in nodular BCC at similar levels, although expression in normal epidermis was negative or weakly basal (Supplementary Fig. S2*A*).

HGF/SF may induce invasive growth through several mechanisms, including regulation of the expression and function of cadherins, integrins, and matrix metalloproteinases (41), and we

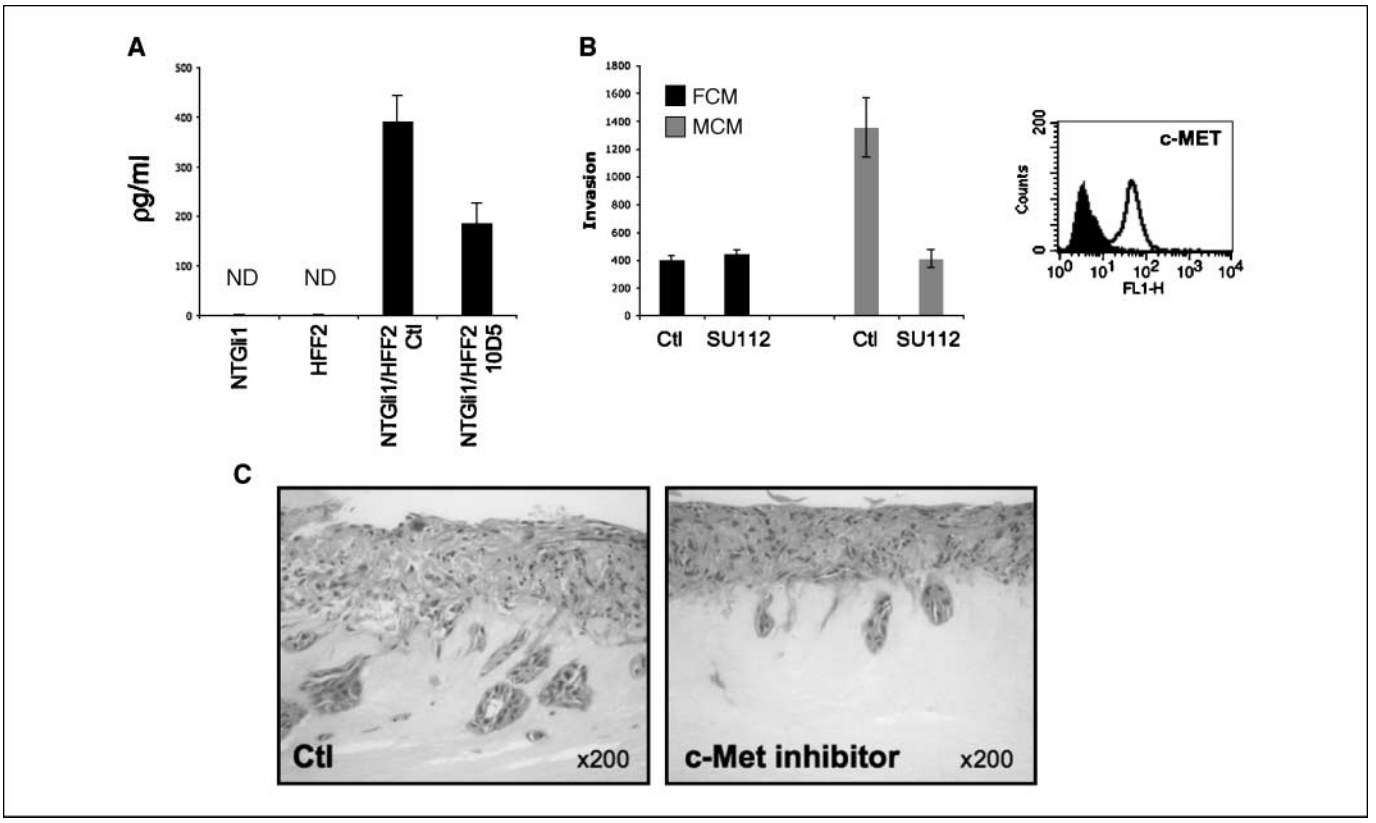

Figure 4. *A,* ELISA showed that HGF/SF was not detectable in NTGli1 or HFFF2 when cultured alone. HGF/SF was up-regulated when NTGli1 and HFFF2 were cocultured and was suppressed when αvβ6 was inhibited using 10D5. *B,* Transwell invasion assay following treatment of NTGli1 cells with Met kinase inhibitor (*SU11274*) and using conditioned medium from fibroblasts (*FCM*) or myofibroblasts (*MCM*) as a chemoattractant. Inactivation of c-Met significantly suppressed the invasion-promoting effect of MCM ($P = 0.00002$). Following c-Met inhibition, the level of invasion was similar to that produced by FCM, suggesting that the invasion-promoting effect of MCM was modulated through HGF/SF. Flow cytometry confirmed c-Met expression by NTGli1 cells. *C,* NTGli1 cells were grown in organotypic culture with HFFF2 cells and treated with Met kinase inhibitor (*SU11274*) or control (vehicle only). Inhibition of c-Met reduced NTGli1 invasion.

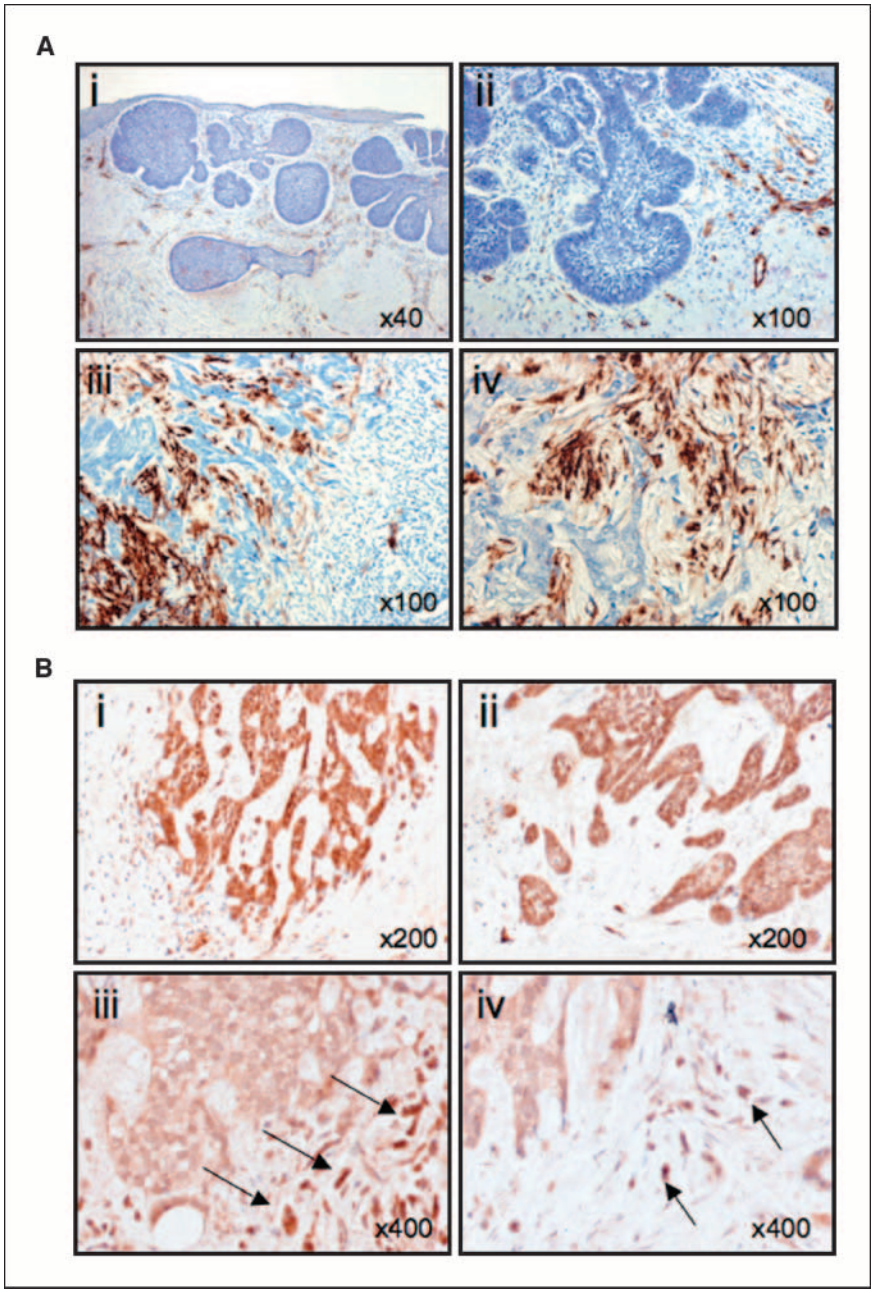

Figure 5. *A,* immunohistochemistry of representative SMA expression in nodular BCC (*i* and *ii*) and morphoeic BCC (*iii* and *iv*). SMA expression was significantly higher in morphoeic BCC ($P = 0.0036$). *B,* immunohistochemistry of representative c-Met (*i* and *ii*) and HGF/SF (*iii* and *iv*) expression in morphoeic BCC. Strong c-Met expression was observed in all tumors. HGF/SF expression was present in stromal cells (*arrows*).

have shown previously that HGF/SF promotes the invasion of head and neck SCC cells (25). Bennett and colleagues showed that HGF/SF induces the expression of type IV collagenases matrix metalloproteinase-2 and matrix metalloproteinase-9 (42), and this observation may suggest a possible mechanism for the HGF/SF-dependent invasion through Matrigel (which is composed predominantly of type IV collagen) described in this study. HGF/SF stimulation also promotes tyrosine phosphorylation of β-catenin, resulting in the loss of E-cadherin binding and nuclear translocation of β-catenin (43). Nuclear localization of β-catenin has been reported to be significantly higher in morphoeic BCC compared with nodular BCC (44). Although Gli1 has been reported to down-regulate E-cadherin expression in BCC through induction of the E-cadherin repressor, Snail (45), immunochemistry showed that E-cadherin expression was maintained in morphoeic BCC (Supplementary Fig. S2*B*). However, there was less membranous and more cytoplasmic staining compared with normal epidermis (Supplementary Fig. S2*B*). These data raise the possibility that altered E-cadherin function may play a role in the morphogenesis of morphoeic BCC, and that this may be modulated through stromal-derived HGF/SF.

In summary, we show that αvβ6 is expressed at significantly higher levels in aggressive morphoeic BCC compared with nodular BCC, and show an indirect invasion-promoting effect modulated through stromal cells; αvβ6-dependent TGF-β1 activation induces a myofibroblastic phenotype resulting in up-regulated HGF/SF secretion which promotes tumor cell invasion. We also confirm that morphoeic BCC are myofibroblast-rich and express HGF/SF and c-Met. These observations from clinically derived material support the suggestion that the paracrine interactions observed

in vitro between BCC cells and fibroblasts may also occur *in vivo*, and might explain the morphologic appearance of morphoeic BCCs. As well as emphasizing the importance of the stromal contribution to tumor development, the data show that αvβ6 may promote tumor invasion through both direct and indirect mechanisms.

Acknowledgments

Received 1/15/2008; revised 2/19/2008; accepted 2/27/2008.

Grant support: Cancer Research UK, The Health Foundation, and the Restoration of Appearance and Function Trust (RAFT). D. Marsh is a RAFT Surgical Research Fellow.

The costs of publication of this article were defrayed in part by the payment of page charges. This article must therefore be hereby marked *advertisement* in accordance with 18 U.S.C. Section 1734 solely to indicate this fact.

References

1. Armstrong BK, Kricker A. The epidemiology of UV induced skin cancer. J Photochem Photobiol B 2001;63:8–18.
2. Wong CSM, Strange RC, Lear JT. Basal cell carcinoma. BMJ 2003;327:794–8.
3. Miller DL, Weinstock MA. Nonmelanoma skin cancer in the United States: incidence. J Am Acad Dermatol 1994;30:774–8.
4. Scrivener Y, Grosshans E, Cribier B. Variations of basal cell carcinomas according to gender, age, location, and histopathological subtype. Br J Dermatol 2002;147:41–7.
5. Dahmane N, Lee J, Robins P, Heller P, Ruiz i Altaba A. Activation of the transcription factor Gli1 and the Sonic hedgehog signaling pathway in skin tumors. Nature 1997;389:876–81.
6. Evangelista M, Tian H, Sauvage FJ. The hedgehog signaling pathway in Cancer. Clin Cancer Res 2006;12:5924–8.
7. Adolphe C, Hetherington R, Ellis T, Wainwright B. Patched1 functions as a gatekeeper by promoting cell cycle progression. Cancer Res 2006;66:2081–8.
8. Oro AE, Higgins KM, Hu Z, Bonifas JM, Epstein EH, Scott MP. Basal cell carcinomas in mice overexpressing Sonic hedgehog. Science 1997;276:817–21.
9. Grachtchouk M, Mo R, Yu S, et al. Basal cell carcinomas in mice overexpressing Gli2 in skin. Nat Genet 2000;24:216–7.
10. Nilsson M, Unden AB, Krause D, et al. Induction of basal cell carcinomas and trichoepitheliomas in mice overexpressing GLI-1. Proc Natl Acad Sci U S A 2000;97:3438–43.
11. Walling HW, Fosko SW, Geraminejad PA Whitaker DC, Arpey CJ. Aggressive basal cell carcinoma: presentation, pathogenesis, and management. Cancer Metastasis Rev 2004;23:389–402.
12. Breuss JM, Gallo J, DeLisser HM, et al. Expression of the β6 subunit in development, neoplasias and tissue repair suggests a role in epithelial remodelling. J Cell Sci 1995;108:2241–51.
13. Thomas GJ, Nystrom ML, Marshall JF. αvβ6 integrin in wound healing and cancer of the oral cavity. J Oral Pathol Med 2006;35:1–10.
14. Munger JS, Huang X, Kawakatsu H, et al. The integrin αvβ6 binds and activates latent TGFβ1: a mechanism for regulating pulmonary inflammation and fibrosis. Cell 1999;96:319–28.
15. Hahm K, Lukashev ME, Luo Y, et al. αvβ6 integrin regulates renal fibrosis and inflammation in Alport mouse. Am J Path 2007;170:110–25.
16. Thomas GJ, Lewis MP, Whawell SA, et al. αvβ6 integrin promotes invasion and migration in squamous carcinoma cells. J Invest Dermatol 2001;117:67–73.
17. Thomas GJ, Lewis MP, Hart IR, Marshall JF, Speight PM. αvβ6 integrin promotes invasion of squamous carcinoma cells through up-regulation of matrix metalloproteinase-9. Int J Cancer 2001;92:641–65.
18. Bates RC, Bellovin DI, Brown C, et al. Transcriptional activation of integrin β6 during the epithelial-mesenchymal transition defines a novel prognostic indicator of aggressive colon carcinoma. J Clin Invest 2005;115:339–47.
19. Nystrom ML, McCulloch D, Weinreb PH, et al. Cyclooxygenase-2 inhibition suppresses αvβ6 integrin-dependent oral squamous carcinoma invasion. Cancer Res 2006;66:10833–42.
20. Elayadi AN, Samli KN, Prudkin L, et al. A peptide selected by biopanning identifies the integrin αvβ6 as a prognostic biomarker for nonsmall cell lung cancer. Cancer Res 2007;67:5889–95.
21. Hazelbag S, Kenter GG, Gorter A, et al. Overexpression of the αvβ6 integrin in cervical squamous cell carcinoma is a prognostic factor for decreased survival. J Pathol 2007;212:316–24.
22. Agrez M, Chen A, Cone RI, Pytela R, Sheppard D. The αvβ6 integrin promotes proliferation of colon carcinoma cells through a unique region of the β6 cytoplasmic domain. J Cell Biol 1994;127:547–56.
23. Janes SM, Watt FM. Switch from αvβ5 to αvβ6 integrin expression protects squamous cell carcinomas from anoikis. J Cell Biol 2004;166:419–31.
24. Dickson MA, Hahn WC, Ino Y, et al. Human keratinocytes that express hTERT and also bypass a p16INK4a-enforced mechanism that limits life span become immortal yet retain normal growth and differentiation characteristics. Mol Cell Biol 2000;20:1436–47.
25. Lewis MP, Lygoe K, Nystrom ML, Anderson WP, Speight PM, Thomas GJ. SCC-derived TGF-β1 promotes myofibroblast differentiation and modulates scatter factor-dependent tumour invasion. Br J Cancer 2004;90:822–32.
26. Regl G, Neil GW, Eichberger T, et al. Human GLI2 and GLI1 are part of a positive feedback mechanism in basal cell carcinoma. Oncogene 2002;21:5529–39.
27. Abe M, Harpel JG, Metz CN, Nunes I, Loskutoff DJ, Rifkin DB. An assay for transforming growth factor-β using cells transfected with a plasminogen activator inhibitor-1 promoter-luciferase construct. Anal Biochem 1994;216:276–84.
28. Nystrom ML, Thomas GJ, Stone M, Mackenzie IC, Hart IR, Marshall JF. Development of a quantitative method to analyse cell invasion in organotypic culture. J Pathol 2005;205:468–75.
29. Tlsty TD, Hein PW. Know thy neighbour: stromal cells can contribute oncogenic signals. Curr Opin Genet Dev 2001;11:54–9.
30. Tuxhorn JA, Ayala GE, Rowley DR. Reactive stroma in prostate cancer progression. J Urology 2001;166:2472–83.
31. Goke M, Kanai M, Podolsky DK. Intestinal fibroblasts regulate intestinal epithelial cell proliferation via hepatocyte growth factor. Am J Physiol 1998;274:G809–18.
32. Kinzler KW, Voglestein B. The GLI gene encodes a nuclear protein which binds specific sequences in the human genome. Mol Cell Biol 1990;10:634–42.
33. Zhou X, Chang Y, Oyama T, McGuire MJ, Brown KC. Cell-specific delivery of a chemotherapeutic to lung cancer cells. J Am Chem Soc 2004;129:15656–7.
34. Van Aarsen LA, Leone DR, Ho S, et al. Antibody mediated blockade of integrin αvβ6 inhibits tumor growth *in vivo* by a TGF-β-specific mechanism. Cancer Res 2008;68:561–70.
35. Elliot RL, Blobe GC. The role of transforming growth factor β in human cancer. J Clin Oncol 2005;23:2078–93.
36. Liotta LA, Kohn EC. The microenvironment of the tumour-host interface. Nature 2001;411:375–9.
37. Pupa SM, Menard S, Forti S, Tagliabue E. New insights into the role of extracellular matrix during tumour onset and progression. J Cell Physiol 2002;192:259–67.
38. De Wever O, Mareel M. Role of tissue stroma in cancer cell invasion. J Pathol 2003;200:429–47.
39. Peruzzi B, Bottaro DP. Targeting the c-Met signaling pathway in cancer. Clin Cancer Res 2006;12:3657–60.
40. De Wever O, Nguyen Q-D, Hoorde LV, et al. Tenascin-C and SF/HGF produced by myofibroblasts *in vitro* provide convergent pro-invasive signals to human colon cancer cells through RhoA and Rac. FASEB J 2004;18:1016–8.
41. Birchmeier C, Birchmeier W, Gherardi E, Vande Woude GF. Met, metastasis, motility and more. Nat Rev Mol Cell Biol 2003;4:915–25.
42. Bennett JH, Morgan MJ, Whawell SA, et al. Metalloproteinase expression in normal and malignant oral keratinocytes: stimulation of MMP-2 and -9 by scatter factor. Eur J Oral Sci 2000;108:281–91.
43. Monga SPS, Mars WM, Pediaditakis P, et al. Hepatocyte growth factor induces Wnt-independent nuclear translocation of β-catenin dissociation in hepatocytes. Cancer Res 2002;62:2064–71.
44. El-Bahrawy M, El-Masry N, Alison M, Poulsom R, Fallowfield M. Expression of β-catenin in basal cell carcinoma. Br J Dermatol 2005;48:964–70.
45. Li X, Deng W, Nail CD et al. Snail induction is an early response to Gli1 that determines the efficiency of epithelial transformation. Oncogene 2006;25:609–21.